Signal Propagation Analysis for Near-Field Intra-Body Communication Systems

[1]Kohei Nagata, [1]Tomonori Nakamura, [1]Mami Nozawa, [1]Yuich Kado, [1]Hitoshi Shimasaki [2]Mitsuru Shinagawa,
[1]Department of Electronics Kyoto Institute of Technology Sakyo-ku Kyoto, Japan
[2]Faculty of Science and Engineering, Hosei University, Koganei-shi, Tokyo, Japan

***Abstract*- We studied MHz-band communication between a TRX on the surface of the human body (wearable TRX) and a TRX embedded in the environment (embedded TRX). In this work, we propose a medical application to take advantage of MHz-band characteristics on the human body by embedding a TRX into the human body (in-body TRX) and examined the feasibility of in- and on-body communication. We also fabricated an electrically isolated probe (E/O-O/E probe) because conventional probes overestimate the received signal due to additional capacitance. The E/O-O/E probe eliminates this additional capacitance and can measure the received signal precisely. We measured the path loss around a phantom equivalent to a human and found that the proposed application is very useful in terms of engineering output power and received sensitivity.**

I. INTRODUCTION

Wireless body area networks around the human body are expected to play an important role in various areas of application [1]. Several recent studies [2]–[6] have focused on body-channel communication (BCC), which is communication between TRXs on the surface of the human body (wearable TRXs) that uses the human body as a communication path. We previously proposed technology for human-area networking based on near field coupling communication (NFCC) using the megahertz band that consisted of wearable TRXs and a transceiver embedded in floors, PCs, and equipment (embedded TRXs) to expand the areas to which BCC can be applied. NFCC can provide more versatile systems than those with BCC and enables intuitive communication because people can touch and connect. There are many advantages to MHz-band communication, including short communication distance, low power consumption, and less absorption of energy for the human body. These characteristics are attractive for various medical applications such as the hospital scenario outlined in Fig. 1. Using wearable TRXs that contain personal information enables medical professionals to know the physical location of patients and the condition of their health. There are also potential applications to security and convenience, e.g., a scenario in which only people who have wearable TRXs can unlock doors by just stepping up to them and walking into an examination room. A TRX embedded in the human body (in-body TRX) collects medical information and communicates with the wearable TRX on the body so that information can be monitored at all times. Moreover, healthcare and medical applications over networks can be combined by using NFCC between an embedded TRX connected to the network and the wearable TRX. When NFCC is applied, medical information leaks can be prevented and the influence on medical equipment and on humans can be limited. It can be used long-term without having to replace batteries.

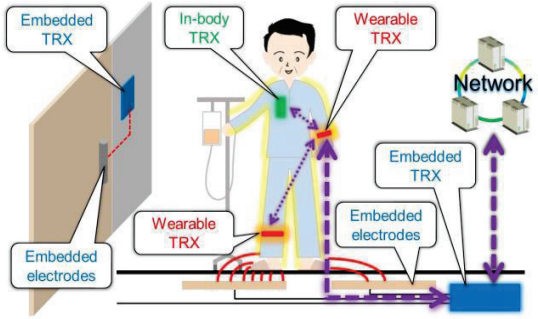

Figure 1. Model of scenario for NFCC application.

II. COMMUNICATION PATH

Figure 2 shows the basic communication model of NFCC between a wearable TRX and an embedded TRX. The signal loop consists of two paths: a forward path and a return path. The forward path runs from the body-side electrode of the wearable TRX through the human body to the upper electrode of the embedded TRX, while the return path runs from the lower electrode of the embedded TRX through the air to the outside electrode of the wearable TRX. When we measure the signal intensity around the human body with the measurement instrument to determine the signal characteristics, an additional path emerges in the equivalent circuit. This makes the return path seem bigger than it is and leads to measurement error.

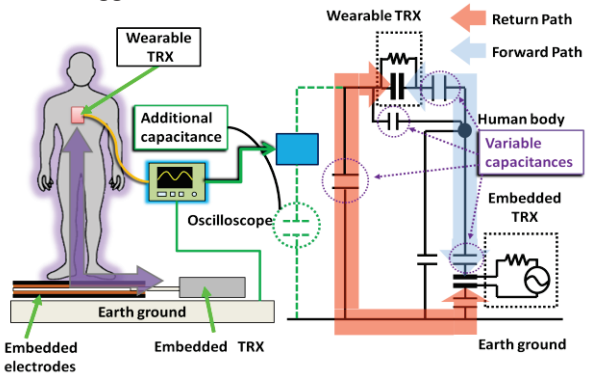

Figure 2. Communication circuit model

III. TRANSCEIVER CONFIGURATION

We fabricated three TRXs —in-body, wearable, and embedded—that could be installed into various objects in

our surroundings, such as doors, floors, and equipment. Figure 3 shows photographs of the configurations for the wearable and in-body TRXs. The prototype used a 6.75-MHz carrier frequency and binary phase-shift keying, achieving a transmission rate of 420 kbps. The wearable TRX was mainly composed of a multi-chip module (MCM), a power circuit, and a coin battery. It could operate for approximately one year on a single CR3032 button lithium-ion battery and incorporated EEPROM that could be used to store user data for applications. The wearable TRX had an asymmetric parallel plate 78 × 49 mm electrode and a horseshoe-shaped electrode to increase space for the button battery**.** We used two different output voltages: an 8-V "Normal V_out" and a 16-V "Double V_out". We measured the packet error rate (PER) using the in-body TRX with two kinds of electrodes, "3*4" types and "card" types, to evaluate the quality of communication between the in-body TRX and the wearable TRX on the human body. The 3*4 electrode was a parallel plate composed of a 3 × 4 cm electrode and the card electrode was the same as the one used in the wearable TRX.

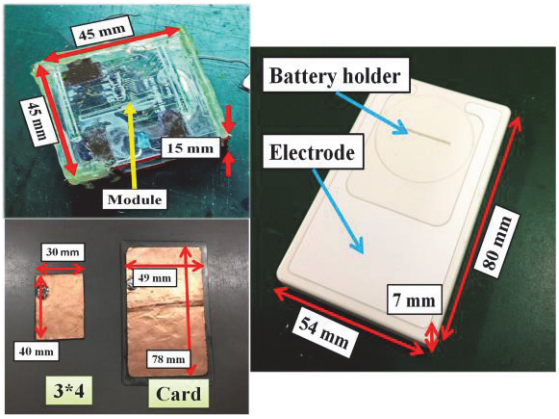

Figure 3. In-body, Wearable TRX configuration and electrodes

IV. Medical Application

A. Experimental system

A schematic of the configuration for the system to measure the PER is shown in Fig. 4. We used a phantom that had the same electrical properties as a human body to ensure the PER measurements could be reproduced. The phantom was made of water-absorbing gel that absorbed a saline solution. Its dimensions were 95 × 19 × 19 cm and its conductivity was 0.59 S/m at 6.75 MHz (human body: 0.60 S/m) [7], which is the carrier frequency of NFCC. The wearable TRX was placed on top of the phantom because it was assumed to be a peripheral device around the body, while the in-body TRX was embedded in the phantom because it was assumed to be a device embedded in the body. The total length of packet data was 22 bytes. Each packet consisted of an address, data, and commands. Ten thousand packets were sent at 1-ms intervals. After all the packets had been sent, we confirmed the number that had been successfully received. We also calculated PER. We measured PER between the in-body and wearable TRXs. When the in-body TRX communicates with the wearable TRX in actual use, there are interspaces between the human body and the wearable TRX such as those resulting from clothes and air space. Polystyrene boards (0–80 mm) were placed between the phantom and the wearable TRX to reproduce this situation and to vary the distance between them. We reproduced the depth at which the in-body TRX was embedded in the human body by varying the embedding depth in the phantom.

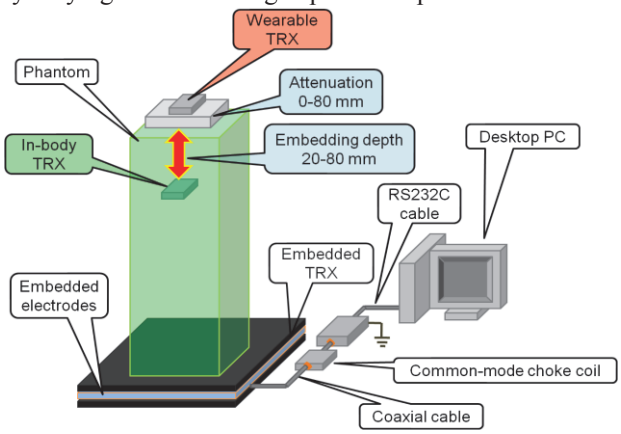

Figure 4. Schematic of PER measurements

B. Results

Figure 5 plots the PER for NFCC from the in-body TRX to the wearable TRX for each electrode. We used double V_out. The solid lines represent the approximate lines for 3*4 electrode and the dotted lines represent those for card electrode. The parameters (20–80 mm) represent embedded depth from the in-body TRX to the surface of the phantom. More stable communication was established when we used a larger electrode with greater distances between the TRXs.

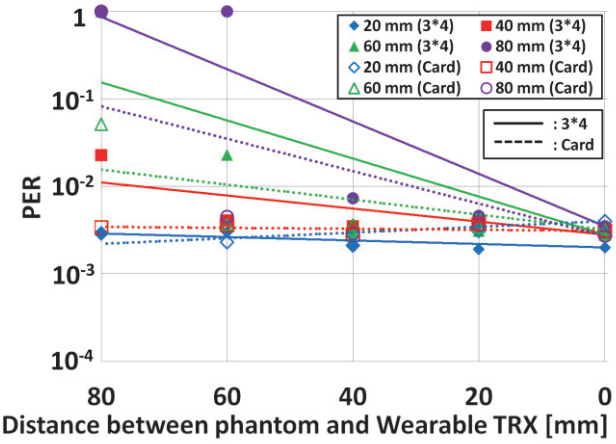

Figure 5. PER from In-body to wearable TRX

Figure 6 plots the PER for communication from the wearable to in-body TRX as parameters of the depth (20–80 mm) for the 3*4 electrode. We only used double V_out TRX because our previous study indicated that communication using a normal V_out TRX was not established in this direction. The PER sharply degraded at a specific distance between the surface and the wearable TRX. For the card electrode, PER was less than 10^{-4}. This means that the signal intensity received by the in-body TRX is a critical factor for PER.

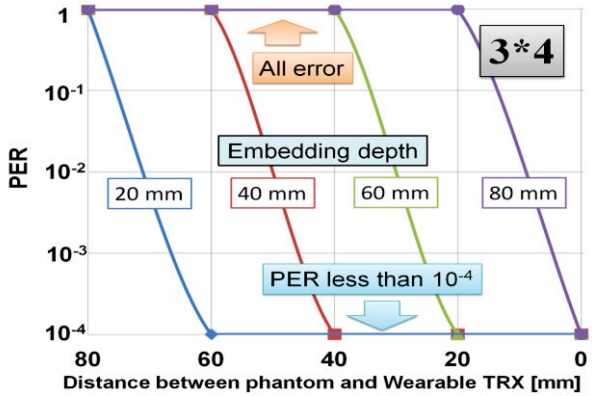

Figure 6. PER from wearable to In-body TRX with 3*4 electrodes

Figure 7 shows the results of the simulation for the electric field distribution around the phantom. The output voltages of the in-body and the wearable TRX were 4.4 V and their signal frequency was 6.75 MHz. The size and the electrical properties of a box placed at the center were the same as those of the phantom. Fig. 7 (a) shows the electrical field generated by the in-body TRX and Fig. 7 (b) shows the electrical field generated by the wearable TRX. As seen in the figures, the range of communication from the wearable to the in-body TRX is narrower than that of backward communication. These results coincide with those we obtained from measurements.

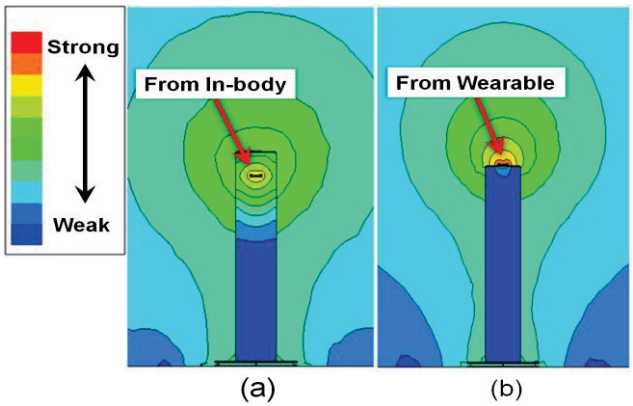

Figure. 7 (a) Electrical distribution from In-body TRX and (b) Electrical distribution from Wearable TRX

V. E/O-O/E

A. E/O-O/E characteristics

Measuring the signal intensity on the human body is very important to determine the output of the TX and the sensitivity of the RX. As discussed in chapter Ⅱ, an additional path appears when we directly measure the signal with a measuring instrument, and we incorrectly measured the signal intensity due to the above. We need a tool to precisely measure the signal intensity on the communication path and to design a stable communication network, so we fabricated the electrically isolated probe and tested it to determine the effectiveness.

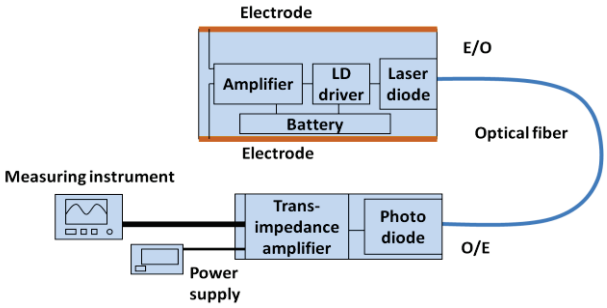

Figure 8. Block diagram of E/O and O/E probe

We measured signal voltages that the probe received when the ground electrode was directly connected to the measuring instrument and when it was not connected. The experimental system is shown in Fig. 9. As the measuring instrument, we chose a battery-operated spectrum analyzer that was independent of the earth grounding. We used two 350-mm-square copper plates as electrodes for the embedded TRX. The distance between the plates was 10 mm. We entered a sine wave of 6.75 MHz by using a signal generator, and the ground electrode of the E/O probe was connected to the spectrum analyzer with a lead line. The ratio between applied and received voltages and changes due to the height of the spectrum analyzer are plotted in Fig. 10. The closer the spectrum analyzer was to the earth ground, the larger the received signals were, as was measured with a conventional electric probe. In contrast, the measured values using the E/O and O/E probe were constant and were not affected by the position of the measuring instrument. In addition, the measured values were much smaller than those obtained with the conventional electric probe because the additional capacitance was excluded from the signal loop by an electrical isolation method. These results revealed that the E/O and O/E probe solved the problem of overestimating the measuring signals and built a repeatable measurement system with the E/O and O/E probe.

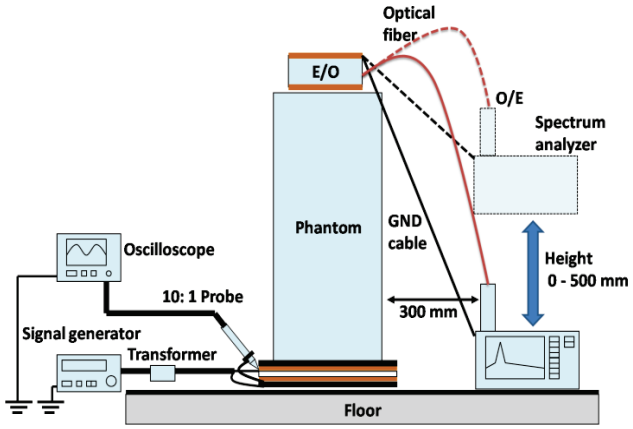

Figure 9. Experimental system to evaluate effect of conventional electric probe on measured value.

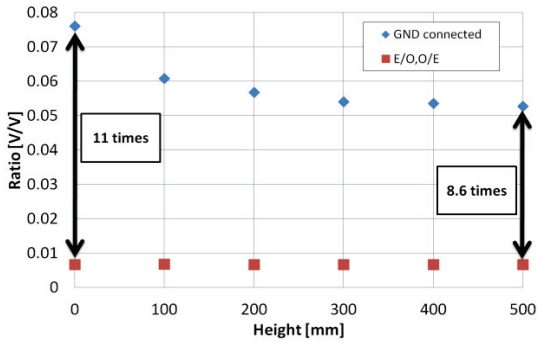

Figure 10. Ratio of applied voltages to received voltages as function of spectrum analyzer height.

B. *Signal distribution around human body*

Figure 11 shows a schematic of the experimental system. We measured the received voltage of the surrounding phantom by using the E/O and electric probes attached to a pole made of PVC pipe placed on wooden rails. This probe was always kept vertical to the ground. We also measured the difference in the potential of the embedded electrodes and provide a graph indicating that the vertical and horizontal attenuation depends on the distance from the phantom (Fig. 12). It is obvious that measuring signals with the electric probe overestimated the signal intensity. As a result, we can precisely confirm the path loss distribution with the E/O probe around the phantom. These results are extremely useful for appropriately determining the receiver sensitivity and transmitter power in order to achieve good communication quality and prevent interference problems in hospital.

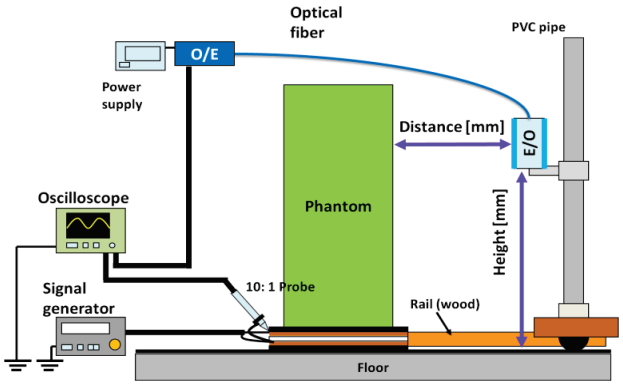

Figure 11. Measuring system for path loss around phantom.

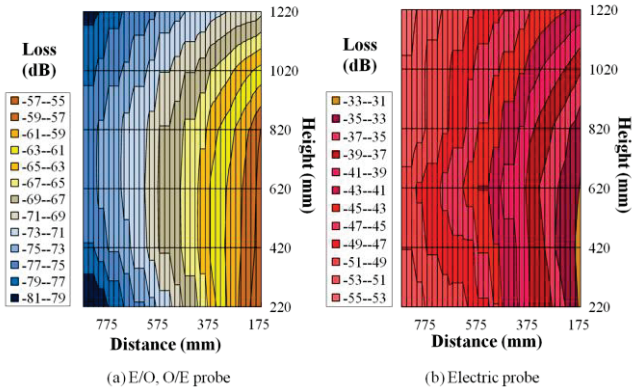

(a) E/O, O/E probe (b) Electric probe

Figure 12. Path loss distribution around phantom.

VI. Conclusion

We applied NFCC to the communication between the inside and outside of the human body and explored the feasibility of this bi-directional communication in order to take advantage of the MHz band. We found that communication can be established and that the size of the electrode is the key factor for determining communication quality. Additionally, through simulation, we found that signal characteristics become altered when TX transmits the signal. To determine the best output power to achieve communication and keep to a minimum influence on the human body or peripheral devices, we fabricated an E/O-O/E probe that eliminates such influence through the measuring instrument. Results showed that it could achieve signal measurement on the human body precisely. In the future, our target is to fabricate the tool for use not only on the body but in the body as well.

Acknowledgment

Part of this work was supported by a Grant-in-Aid for Scientific Research (A) 23246073 from the Ministry of Education, Culture, Sports, Science and Technology of Japan.

References

[1] N. Cho, J. Yoo, S. J. Song, J. Lee, S. Jeon, and H. J. Yoo,"The Human Body Characteristics as a Signal Transmission Medium for Intrabody Communication," *IEEE Trans. Microwave Theory and Techniques,* Vol. 55, pp. 1080-1086, May 2007.

[2] A. Fazzi, S. Ouzonov, and J. v. d. Homberg,"A 2.75mW Wideband Correlation-Based Transceiver for Body-Coupled Communication," *IEEE ISSCC,* pp. 204-205, Feb 2009.

[3] J. Bae, H. Cho, K. Song, H. Lee, and H. J. Yoo, "The Signal Transmission Mechanism on the Surface of Human Body for Body Channel Communication," *IEEE Trans. Microwave Theory and Techniques,* Vol. 60, pp. 582-593, March 2012.

[4] T. G. Zimmerman, "Personal Area Networks: Near-field intrabody communication," *IBM Syst. J.* , Vol. 35, no. 3--4, pp. 609--617, 1996.

[5] Y. Kado and M. Shinagawa, "AC Electric Field Communication for Human-Area Networking," *IEICE Trans. Electron.*, Vol.E93-C, pp. 234-243, MAR 2011

[6] A. Fazzi, S. Ouzonov, and J. V. D. Homberg, "A 2.75 mW Wideband Correlation-Based Transceiver for Body-Coupled Communication," IEEE ISSCC, pp. 204–205, Feb. 2009.

[7] S.Gabriel, R.W.Lau and C.Gabriel, "The dielectric properties of biological tissues: Ⅱ.Measurements in the frequency rage 10 Hz to 20 GHz", Phys. Med. Biol. Vol.41, pp.2251-2269 ,1996

[8] Y. Kado, T. Kobase, T. Yanagawa, T. Kusunoki, M. Takahashi, R. Nagai, O. Hiromitsu, A. Hataya, H. Shimasaki, and M. Shinagawa : "Human-Area Networking Technology Based on Near-Field Coupling Transceiver" *2012 IEEE Radio & Wireless Sym. (RWS 2012),* pp. 119 - 122, Santa Clara, California, USA, Jan. 2012.

[9] K. Nagata, Y. Kado : "Transmission Characteristics between In-body and On-body Transceivers Using MHz-band Near-field Coupling Technology" *7th International Symposium on Medical Information and Communication Technology,* pp 71-75, Tokyo, Japan, Mar, 2013

[10] M. Nozawa, T. Nakamura, H. Simasaki, Y. Kado and M. Shinagawa, "Signal Measurement System Using Electrically Isolated Probe for MHz-Band Near-Field Coupling Communication", *IEEE International Instrumentation and Measurement Technology Conference 2013, pp. 37 – 40,* Minneapolis, MN, USA, May. 2013.